ECS Transactions, 57 (1) 959-967 (2013)
10.1149/05701.0959ecst ©The Electrochemical Society

Sol-Gel Thin-Film Electrolyte Anode-Supported SOFC – From Layer Development to Stack Testing

Norbert H. Menzler, Feng Han, Doris Sebold, Qingping Fang, Ludger Blum and Hans Peter Buchkremer

Institute of Energy and Climate Research – IEK, Forschungszentrum Jülich, 52425 Jülich, GERMANY

One of the current R&D projects on solid oxide fuel cells concerns the reduction of the operation temperature. Nowadays stacks with anode-supported cells and an LSCF-cathode operate typically at a mean temperature of 700°C. The minimum temperature for SOFC using natural gas is approx. 650°C due to reforming limitations. Reducing temperatures below 600°C leads to lower costs, shorter start-up time and thus in-time power delivery by the system (e.g. for auxiliary power units). Forschungszentrum Jülich is also working on the development of an SOFC operating at 400°C for special applications, which can be fueled either with hydrogen (produced by, for example, electrolysis using renewable energy) or with reformate gas based on, for instance, ethanol/methanol. The main challenge for using the SOFC at such low temperatures is, besides electrode activities, overcoming the resistances, especially the ohmic resistance of the electrolyte. This can be achieved in two ways: by introducing materials which show higher oxygen diffusivity or by using the classical materials and minimizing the electrolyte thickness down to values below 2µm.

Introduction

One of the main achievements of solid oxide fuel cell R&D in the last 20 years has been the reduction of the operating temperatures. This applies for any type of SOFC such as tubular cathode-supported SOFCs (Westinghouse, Siemens), which started at operating temperatures of about 950°C and finally operated at around 850°C (1). The same direction was taken with planar electrolyte-supported cells whose operating temperatures have been reduced to currently 850°C (2). And, finally also anode-supported planar cells and stacks, which first operated at around 800°C by using a classical La-Sr-Mn-based cathode, and successively reached typical operating temperatures of 700°C (3). The main reason for this temperature reduction for all SOFC types is extending the lifetime by reducing the degradation effects governed by energetically driven effects. Thus by reducing operating temperature also degradation effects become reduced/slower and therefore the lifetime of the system can be enhanced.

However, if the energetically driven degradation effects are minimized by temperature reduction, every electrochemical process within the SOFC is also slowed down simultaneously. In other words, by reducing the temperature also the current

density and the power density of the cell/stack will be reduced as well (these effects are the two sides of the same coin).

There are two possible ways to ensure high power output despite reduced temperature:

- introducing novel materials for the electrolyte and/or the electrodes (depending on the power-limiting component) to enhance kinetics, ionic or electronic conduction, and catalysis, or
- minimizing the electrolyte thickness to reduce the ohmic resistance or nanostructuring of the electrodes to enhance the triple phase boundaries

The development of novel materials continues, with time-consuming efforts. In many cases, the novel materials demonstrated improved electrochemical activity, but also showed disadvantages with respect to, for example, material interaction, costs, workability, and sinterability. Irrespective of all these rather negative implications, novel materials with balanced properties have to be developed in order to further reduce operating temperatures in SOFCs.

On the other hand, nanostructured electrodes can help to enhance the electrochemical kinetics and current density. However, some manufacturing steps during cell fabrication (e.g. electrolyte sintering at T > 1300°C) and stack start-up (sealing at T ≥ 850°C for a long time) often change the nanostructure into a microstructure leading to strong degradation during the first hours of stack operation (and reaching at least the same power level as the micro-sized component). Thus, if nanostructured electrodes are to be used, also the electrolyte has to be applied by low-temperature techniques (e.g. physical vapor deposition, sputtering, plasma spraying, electrophoresis) and even stack start-up and operating temperature levels have to be minimized.

Thus R&D work at Forschungszentrum Jülich for SOFCs operating at reduced temperature has been focused on reducing the electrolyte thickness assuming that the ohmic resistance of the electrolyte is the rate-limiting step of the overall electrochemical reactions (4). In the first approach, conventional materials for the classical “thick-film” electrolyte ASC (anode-supported cell) were applied.

Cell Manufacturing

By using the sol-gel and nanosuspension technique, very thin electrolyte layers (~ 1µm) were prepared on standard-type tape-cast supports (NiO (Mallinckrodt Baker) and 8YSZ (with 8 mol% yttria-stabilized zirconia; UCM)) (5) and anodes (NiO and 8YSZ (Tosoh)). Subsequently, a similarly thin barrier layer composed of CGO was applied (physical vapor deposition, PVD). Finally, an LSC (La-Sr-Co-oxide) or LSCF (La-Sr-Co-Fe-oxide, both produced in-house) cathode was screen printed and sintered or non-sintered. The power density of such single cells can reach 1.4 W/cm² at 0.7V (600°C, H_2) (6).

In Figure 1, a SEM cross section presents the microstructure of such cells in comparison to a classical LSCF cathode-based cell.

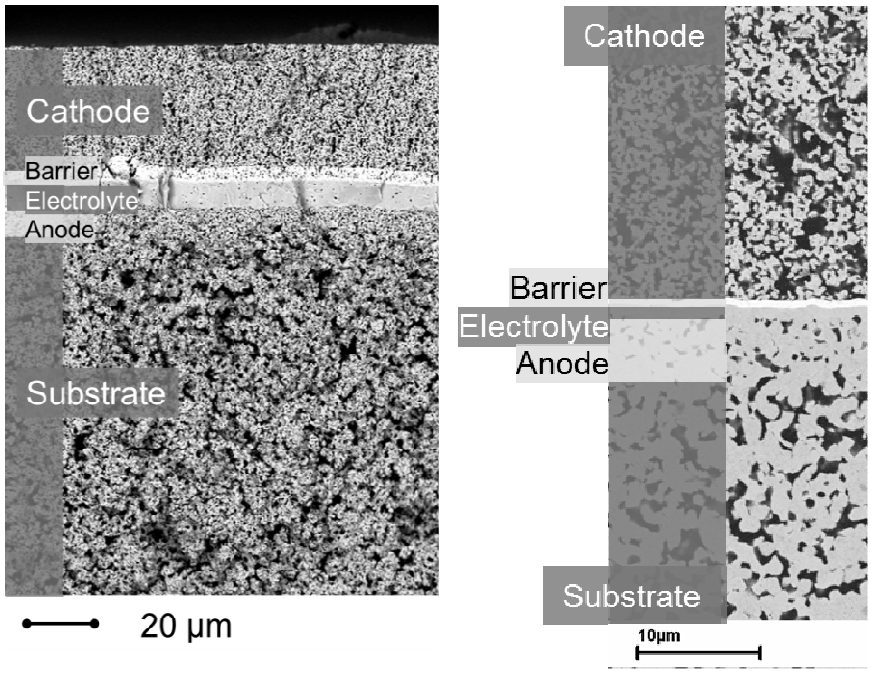

Figure 1. SEM cross sections of a standard type ASC cell (left) and a cell with thin-film sol-gel electrolyte and thin-film barrier applied by PVD (right) (note the different magnifications)

With proven manufacturing reproducibility of such types of cells and homogeneity of all layers and physical parameters (e.g. leak rate and thickness), larger cells of 100x100mm² were prepared (with LSCF cathode) in the same way for a short stack to characterize the manufacturability, handlability, and usability in a stack environment, and to prove whether the good single cell results can be reproduced and transferred to the stack level.

Stack Testing

A four-plane stack was assembled and delivered 0.9 A/cm² at 650°C with H_2/20% H_2O (F_U ~ 25%). The calculated area-specific resistance was 170 and 440 mΩ cm² at 800° and 650°C, respectively. This value is the lowest ASR ever measured for Jülich F-design stacks. On the cathode compartment side of the stack, the interconnect and the metal frame were coated with a chromium evaporation protection layer (Mn oxide) and a cathode contact layer (LCC10) by wet powder spraying. A glass-ceramic was used for the interconnect and the cell sealing, (7). Stack sealing was performed at 850°C for 100h to carefully crystallize the glass and to enhance gas tightness of the sealant. Afterwards the cells were reduced and I-V-curves were measured at various temperatures (800-650°C) (Fig. 2). The stack was operated for approx. 1300h at 700°C and for 1200h at 600°C (Fig. 3).

The calculated mean voltage degradation rate over the entire operating time of 2,500h ranges from 2.1 to 5.7 %/1,000h. This is somewhat higher (factor of 2-6) than expected and higher than measured for comparable stacks (without the sol-gel electrolyte)

(8). However, even at a low operating temperature of only 600°C the cells still deliver 620-680 mV at a current density of 500 mA/cm². This first stack result shows that such types of cells can be operated under relatively low temperatures by maintaining good power density (fueled with hydrogen).

After 2,500h, the stack was shut down in a controlled manner and carefully post-test analyzed. The main goal of the post mortem analysis was to find out why the stack degradation was higher than that of comparable stacks and higher than expected.

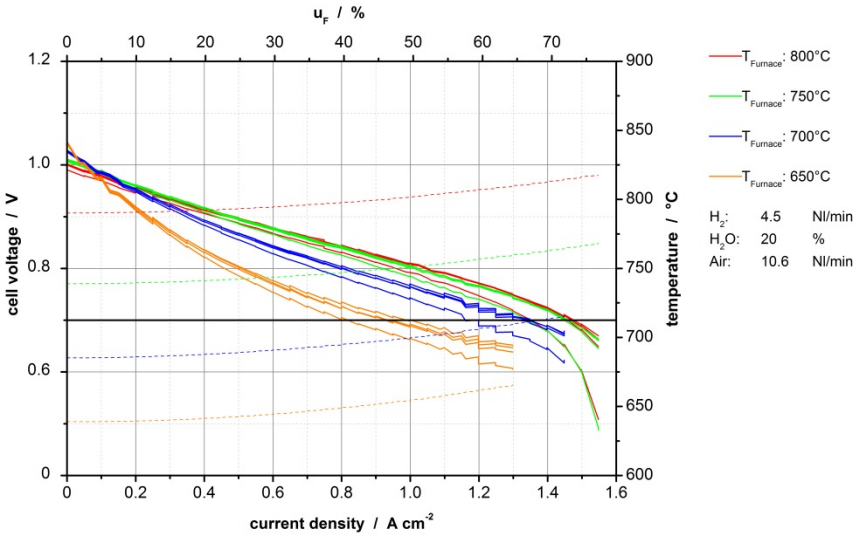

Figure 2. I-V-curves of the stack F 1004-35 between 800 and 650°C

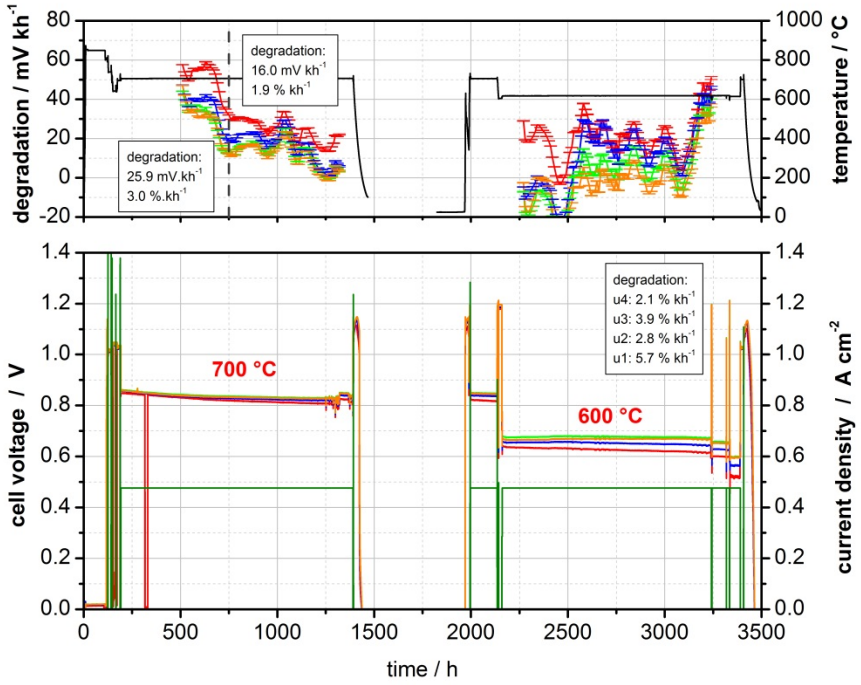

Figure 3. Voltage, current density, temperature and degradation plot of the four-plane stack with sol-gel electrolyte ASCs (the interruption was due to a failure in the anodic mass flow controller)

Stack Dissection and Post-Test Analysis

Stack dissection was performed according to internal standards and protocols (9). Firstly, all planes were removed layer-by-layer, photographed from both sides and stored. Afterwards, one cell (plane 2) was dismantled from the metallic frame and three pieces each 10x10mm² in size were cut removed by laser cutting. Two of them (Nos. 1, 2) were used for wet chemical chromium analysis to compare the amount of Cr incorporated into the cathode to previous results (10), and the third one was used for SEM characterization (Fig. 4). The sample was embedded in a polymeric resin, ground and polished. Samples No. 1 and 2 were prepared according to (11) and the amount of chromium was analyzed by ICP-OES (inductively coupled plasma – optical emission spectroscopy).

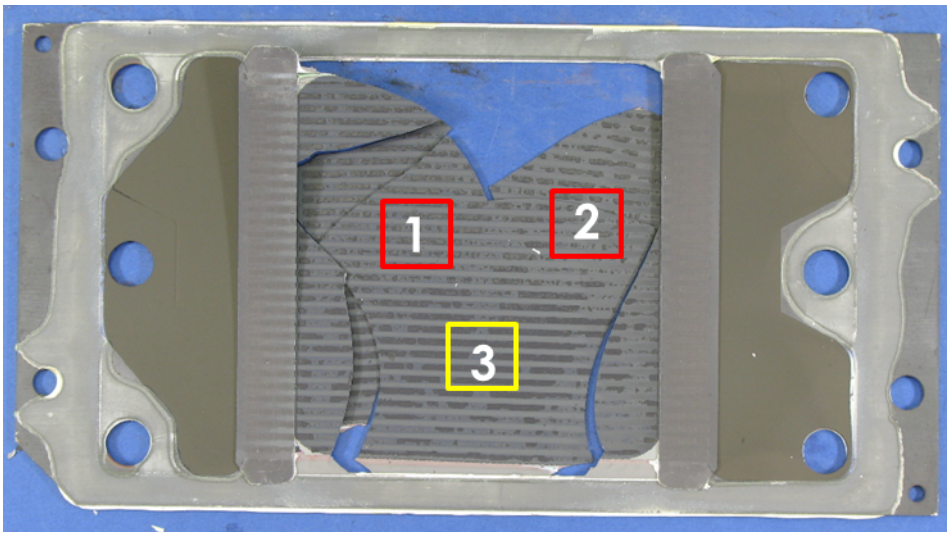

Figure 4. Top view of the cathode side of plane 2 of stack F 1004-35; the squares mark the laser-cut cell samples (red, Nos. 1 and 2 for wet chemical analysis, yellow, No. 3 for SEM; cell broke during stack dissection)

The amount of chromium analyzed was 22-71 µg/cm², which is a normal amount for such operating times (10) (typically the reduced temperature does not strongly influence chromium evaporation).

According to (12), the interaction between volatile chromium species and LSCF cathodes takes place at the surface of the cathode (in contrast to the interaction with LSM-based cathodes, where a manganese-chromium spinel is formed at the border between cathode and electrolyte (10)). The interaction of Cr species and the LSCF cathode leads to the formation of a Sr-Cr-oxide. It is found that the foreign phase formation only takes place at the top surface underneath the contact area of the interconnect bars, growing into the cathode contact layer. No foreign phase remnants could be detected at the top surface of the cathode in the channel. Both species, the volatile chromium oxyhydroxide and also presumably a volatile Sr species, were transported with the air stream outside the stack. Only in those regions where the air flow is limited (within the contact layer) does the foreign phase precipitate. Taking these findings into account, chromium-containing remnants were scanned.

Figure 5 shows an SEM overview of cross sections of the selected cell.

As can be seen from Fig. 5, the cell sample was cut and polished crosswise to the gas channels and therefore also the contact layer can be characterized. The overview pictures do not reveal any special details. As is typical of the LSCF cathode, some cracks formed during drying and sintering due to the mismatch in thermal expansion coefficient between LSCF and 8YSZ/anode substrate. However, all layers appear to be acceptable, uniform and homogeneous.

Afterwards, the analysis focused on the chromium-containing foreign phases which should have formed at the boundary to the contact layer. Very small amounts of Cr-containing phases were found erratically distributed over the entire border region (Fig. 6). Based on the Cr amount measured by wet chemical analysis, more foreign phases would have been expected and should have been detected in this area. Surprisingly, only trace amounts of chromium were detected by EDX point analysis.

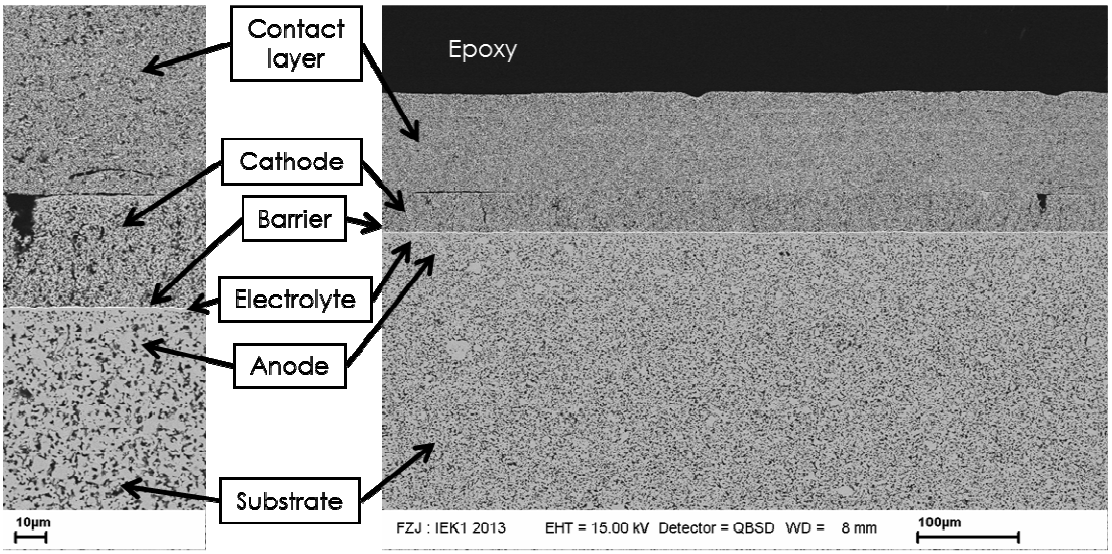

Figure 5. SEM cross section of the dismantled, embedded and polished cell sample; right: overview, left: higher magnification of the functional layers

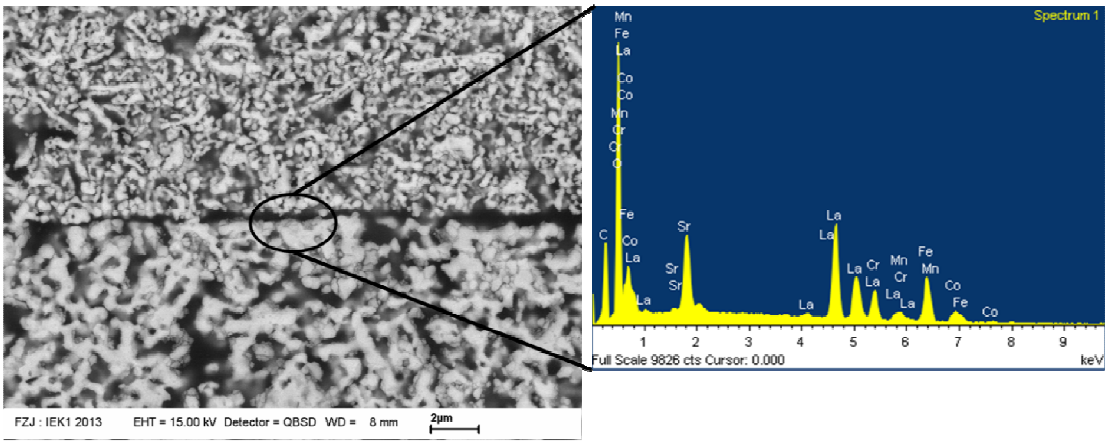

Figure 6. SEM cross section of the borderline cathode/contact layer (left) and EDX spectrum (right) of position 1 marked in the SEM picture

After sample characterization, microstructural changes were also observed at the borderline between the cathode and the CGO barrier layer (Fig. 7), and another foreign phase containing Cr was found at the borderline. In the EDX spectrum, all elements of the cathode (La, Sr, Co, Fe) and the barrier layer (Ce, Gd), as well as Cr, can be detected. However, it was not possible to obtain more information to determine exactly which foreign oxide phases were formed in this area with EDX, because the grain/domain size of the foreign phases is too small in comparison to the interaction volume of the SEM electron beam. Thus, different phases cannot be distinguished in this area.

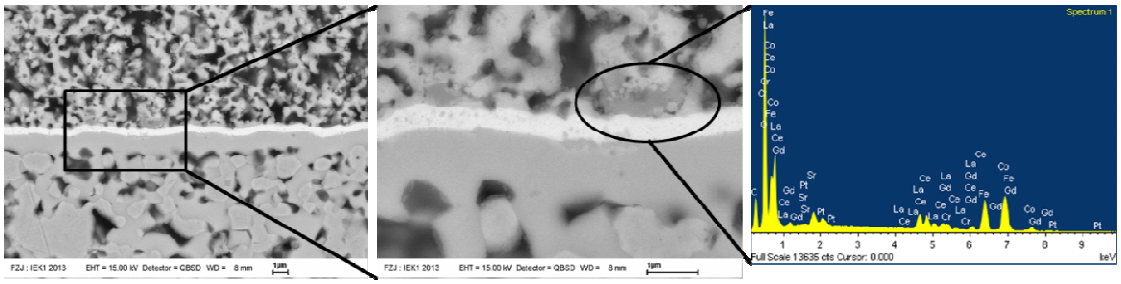

Figure 7. SEM cross sections and EDX spectrum of point analysis No. 1 (left: overview, middle: higher magnification of analyzed area, right: EDX spectrum of area No. 1)

This result shows for the first time that a chromium-containing foreign phase forms during stack operation of anode-supported cells with an 8YSZ thin-film electrolyte, a CGO barrier layer applied by PVD and a screen-printed LSCF cathode. No reference in the literature has found up to now with comparable results: neither with a PVD CGO layer applied on top of a thick (10µm) screen-printed 8YSZ electrolyte, nor within cells having a screen-printed 8YSZ electrolyte and a screen-printed CGO layer, nor in pure CGO-containing electrolyte (without 8YSZ).

The main difference between the cells characterized in the literature and that investigated in this study is the thin-film electrolyte. As the thin-film electrolyte drastically reduces the ohmic resistance of this layer (6), it might be speculated that also the electrochemically driven redox potentials on the three phase boundaries change. In the case of LSM cathodes, beyond a current density threshold the reduction of the volatile Cr-VI species to solid Cr-III species promotes oxygen reduction (10) and therefore the cell degrades during the first few hundred hours of operation. In the case of LSCF, until now only the formation of the less conducting Sr-Cr-oxide has been found. This foreign phase forms independently of the electrochemistry and inhibits electron conduction between the cathode and contact layer, leading finally also to degradation. However, typically the redox potential at the border of the cathode/barrier layer does not promote Cr reduction and subsequent foreign phase formation. This seems to be changed if a thin-film electrolyte is used.

The fundamental explanation for these findings remains to be clarified in future using specially detailed single-cell test housings with defined Cr partial pressure tests and at varying current load. The determination of the formed phase (composition) has to be characterized by additional TEM studies.

Moreover, it is observed that the second phase also shows closed porosity within the CGO layer (not shown here). Whether this type of porosity is connected to foreign

phase formation, whether it is a result of this reaction or whether there is some other reason for it is still unclear.

Finally, no interdiffusion phenomena were found between the anode and the cathode (Ni in cathode, La, Sr, Co, Fe in the anode), thus confirming the gas tightness and diffusion blocking of the electrolyte and the barrier layer for the tested operational conditions.

Conclusions

The thin-film electrolyte for SOFCs was prepared by nanosuspension and the sol-gel method while all other layers were standardized. Anode-supported single cells with a 1µm thin 8YSZ electrolyte, a 1µm thin barrier layer and an LSC cathode deliver 1.4 W/cm² at 0.7V (600°C, H_2) in single cell tests. Furthermore, a four-plane stack with cells of 100x100mm² size was manufactured and tested using comparable cells but with an LSCF cathode. The current density at 650°C was 0.9 A/cm² with H_2/20% H_2O (F_U ~ 25%). The calculated area-specific resistance was 170 and 440 mΩ cm² at 800° and 650°C, respectively. The stack was operated for approx. 1300h at 700°C and for 1200h at 600°C. Cell development, electrochemistry and post-test characterization were presented. The stack degradation was enhanced by a factor of 2-6 compared to similar stacks with a thick-film electrolyte (10µm). Stack and cell post-test analysis shows no overall microstructural changes in the cell, but Cr-containing foreign phases were found at the typical boundary cathode/contact layer and also another foreign phase which contains Cr at the boundary cathode/barrier layer. The latter was unexpected and found for the first time. The foreign phase formation may explain the higher degradation of this stack. The reason for the formation of such types of phases and the conditions under which they are formed remains to be evaluated in future.

Acknowledgements

The authors gratefully acknowledge support from the cell manufacturing group at IEK-1, the stack assembly group of ZEA-1, and the wet chemical analysis by H. Lippert from ZEA-3.

References

1. DiGiuseppe G.: High power density cell development at Siemens Westinghouse. Electrochem. Soc. Proc. Vol. 2005-07, The Electrochem. Soc., Pennington, NJ, USA (2005), 322-332
2. Megel S., Kusnezoff M., Trofimenko N., Sauchuk V., Michaelis A., Venskutonis A., Rissbacher K., Kraussler W., Brandner M., Bienert C. and Sigl L.S.: *High-efficiency CFY-stack for high power application. ECS Transactions* **35** (1), 269, (2011).
3. de Haart L.G.J. and Vinke I.C.: *Long-term operation of planar type SOFC stacks. ECS Transactions* **35** (1), 187 (2011).

4. Ivers-Tiffée E., Hayd J., Klotz D., Leonide A., Han F. and Weber A.: *Performance analysis and development strategies for solid oxide fuel cells. ECS Transactions* 35 (1), 1965 (2011).
5. Schafbauer W., Menzler N.H. and Buchkremer H.P.: Tape casting of anode supports for solid oxide fuel cells at Forschungszentrum Jülich. Int. J. Appl. Ceram. Technol.. http://onlinelibrary.wiley.com/doi/10.1111/j.1744-7402.2012.02839.x/pdf
6. Han F., Mücke R., van Gestel T., Leonide A., Menzler N.H., Buchkremer H.P.and Stöver D.: Novel high-performance solid oxide fuel cells with bulk ionic conductance dominated thin-film electrolytes. *J. Power Sources.*, **218**, 157 (2012).
7. Gross S.M., Federmann D., Remmel J. and Pap M.: Reinforced composite sealants for solid oxide fuel cell applications. *J. Power Sources*., **196** (17), 7338 (2011).
8. Blum L., de Haart L.G.J., Malzbender J., Menzler N.H., Remmel J. and Steinberger-Wilckens R.: Recent results in Jülich solid oxide fuel cell technology developments. J. Power Sources accepted
9. Menzler N.H. and Batfalsky P.: Post-test characterization of solid oxide fuel cell stacks. In Fuel Cells: Science and Engineering Materials, Systems, Processes and Technologies. Edited by Stolten D., Emonts B. Chapter 16, Wiley-VCH, p.469, (2012).
10. Menzler N.H., Vinke I. and Lippert H.: Chromium poisoning of LSM cathodes – results from stack testing. ECS Transactions **25**/2, 2899 (2009).
11. Neumann A., Menzler N.H., Vinke I. and Lippert H.: Systematic study of chromium poisoning of LSM cathodes – single cell tests. ECS Transactions **25**/2, 2889 (2009).
12. Menzler N.H., Batfalsky P., Groß S.M., Shemet V. and Tietz F.: Post-test characterization of an SOFC short stack after 17,000 hours of steady operation. ECS Transactions **35** (1), 195 (2011).